

Fine structure of symmetric grain boundaries in tungsten

P. A. Berezhnyak, O. A. Velikodnaya, T. I. Mazilova, and I. M. Mikhallovskii
*Kharkov Physicotechnical Institute, National Science Center, 310108 Kharkov,
The Ukraine*

(Submitted 28 February 1994)

Pis'ma Zh. Eksp. Teor. Fiz. **59**, No. 8, 515–519 (25 April 1994)

Oscillatory features have been found in the variation of the atomic density near symmetric grain boundaries by field ion microscopy and numerical simulation.

Substantial progress has been made in the description of the structure of grain boundaries in metals in recent years thanks to the development of high-resolution electron microscopy and numerical-simulation methods.¹⁻³ It has been established that the structural width of a grain boundary, i.e., of the region in which the lattices undergo reorientation and in which the cores of grain-boundary lattice defects are concentrated, is $(1-2)a$, where a is the lattice constant. Several physical properties, in particular, the absorption capability of the boundaries, are determined by structural features of the cores of grain boundaries.⁴ Analysis of data on the diffusive penetrability of grain boundaries shows that the region outside the core also has properties which differ from the bulk properties⁵ and which cannot be described in terms of long-range stress fields of grain-boundary dislocations.

There is a quantitative correlation between (on the one hand) the energy of the boundaries and several other properties and (on the other) the extent of the grain-boundary dilatation.³ In theoretical work on the structure and properties of grain boundaries it is usually assumed that the grain boundaries are regions with an excess volume localized in a region corresponding to the width of the core of the boundary.^{3,6} In this letter we are reporting an analysis of grain-boundary features in the atomic density carried out by high-resolution, low-temperature field ion microscopy and numerical simulation. We have observed oscillations in the local density in a region much larger than the width of the core of the boundary.

Large-angle grain boundaries were studied in acicular bicrystals prepared by electrochemical etching of a textured tungsten wire 99.98% pure. The experiments were carried out in a field ion microscope in which the samples were cooled with liquid hydrogen. Helium at a pressure of 10^{-3} Pa was used as the imaging gas. Information on the atomic structure of the boundary region was found through an analysis of the configuration of atomic steps formed during a controlled layer-by-layer low-temperature field evaporation. The smallest thickness of an evaporated layer corresponded to the interplanar distance for planes with large Miller indices (~ 0.01 nm). The deep cooling of the test samples and the use of the method of controlled atom-by-atom evaporation resulted in a resolution at the atomic scale over the entire field of the image. It was thus possible to carry out a detailed study of the structure of the boundary regions.

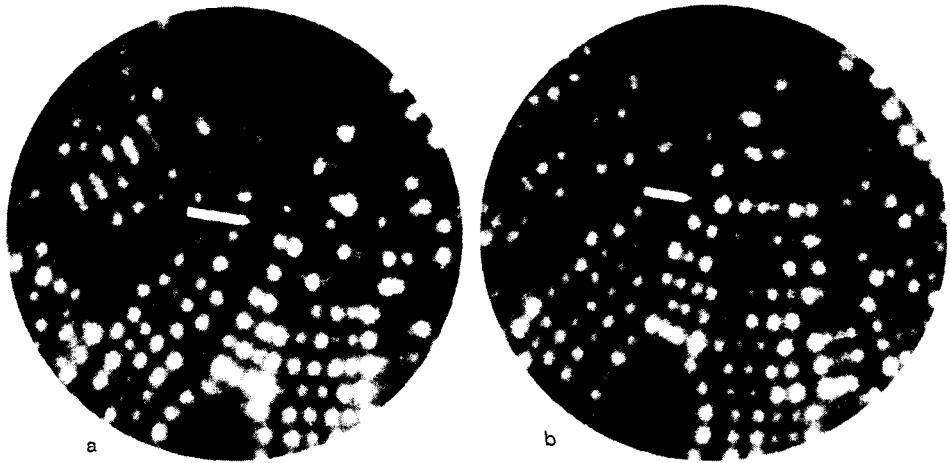


FIG. 1. Change in the grain-boundary contrast on an ion micrograph of a large-angle grain boundary (marked by arrows) during evaporation. The stages of the evaporation corresponding to the formation of the track of the boundary take the following form: a—band with a reduced atomic density; b—a close-packed chain of atoms.

The cores of most of the large-angle boundaries have a reduced density and exhibit a tendency toward a preferential field evaporation.⁷ This effect is seen, in particular, in a decrease in the surface density of the imaged atoms along the track of grain boundaries (Fig. 1a). An inversion of the contrast was observed in certain stages of the evaporation of atoms near certain special boundaries. Close-packed atomic chains of elevated brightness, oriented along the track of a boundary, were observed (Fig. 1b). Analysis of series of ion micrographs recorded in succession during atom-by-atom field evaporation showed that local planar boundary regions with an elevated density may be responsible for the occurrence of a chain of atoms with an elevated brightness. Shown for comparison in Fig. 2 is a model image of a bicrystal containing a $\Sigma 9$, $(1\bar{1}4)$, $\theta=38.9^\circ$ [110] boundary, where Σ is the inverse density of coincident sites, and θ is the misorientation angle. A numerical simulation was carried out in the approximation of a geometric model of thin shells.⁷ One of the atomic planes oriented parallel to the plane of the boundary has a doubled atomic density. Close-packed chains of atoms in the model images were observed during the stages of the field evaporation corresponding to a coincidence of the surface atomic steps with the track of the plane of the double-density boundary. The change in the local packing density of atoms observed during the field evaporation (Fig. 1) stems from a displacement of an atomic step near a boundary.

Although a correspondence between the actual and model ion micrographs could be established in several cases, further work was required to confirm that there are regions with an elevated planar atomic density in addition to regions with an elevated local dilatation at boundaries.⁵ Accordingly, a numerical simulation of the atomic structure of a $\Sigma 9$, $(1\bar{1}4)$, $\theta=38.9^\circ$ [110] boundary was carried out by the method of molecular dynamics. The binary central potential developed for tungsten by Johnson

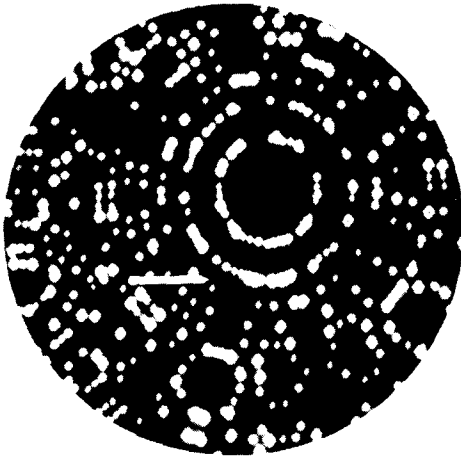


FIG. 2. Model image of a bicrystal containing a $\Sigma 9$ symmetric grain boundary. The arrow marks a close-packed group of atoms at the boundary.

and White⁸ was used as the potential for the interatomic interaction. The model crystallite contained $\sim 10^3$ atoms. Three periods along the $[110]$ direction (six atomic planes) were taken into account. As in Ref. 2, some flexible boundary conditions were imposed at the planes which bound the crystallite and which are parallel to the $[110]$ direction. Cyclic boundary conditions were imposed at the (110) surface planes. A configuration with a minimum energy was found after a rigid relative translation of the lattices by 2.6 \AA along the plane of the boundary, perpendicular to the misorientation angle, and 0.5 \AA in the direction perpendicular to the plane of the boundary. Pentagonal bipyramids can be used as structural elements at a grain boundary.

Figure 3 shows the structure of $\Sigma 9$, $(1\bar{1}4)$, $\theta=38.9^\circ$ $[110]$ grain boundaries in projections onto the (110) plane (a) and the $(1\bar{1}4)$ plane (b). The local grain-boundary dilatation of the boundary region is oscillatory: The distance (d) between neighboring $(1\bar{1}4)$ atomic planes parallel to the boundary varies in a nonmonotonic way (Fig. 4). The atomic planes of the adjacent crystals ($d \approx 0$) merge completely at the center of the core of a boundary, causing a plane with a doubled planar density, $2(1\bar{1}4)$, to form (Fig. 3b).

In contrast, the distance to the atomic planes nearest the core is much larger than the $(1\bar{1}4)$ interplanar distance in the interior of the crystal. This region also dominates the grain-boundary dilatation. Planar oscillations of the atomic density are observed out to 12–15 interplanar distances, i.e., in a region an order of magnitude greater than the half-width of the boundary core.

A numerical simulation of a 2D lattice was carried out to distinguish the contribution of the near-boundary atomic planes to the formation of the atomic configuration of the boundaries. The interaction potential and the boundary conditions used here were the same as those used in the solution of the 3D problem. The initial configuration corresponded to a close-packed $2(1\bar{1}4)$ grain-boundary plane. After relaxation, the $2(1\bar{1}4)$ 2D lattice configuration remained essentially the same. The only changes which could be observed were some slight excursions of atoms from positions corresponding to the sites of a $2(1\bar{1}4)$ close-packed grain-boundary plane.

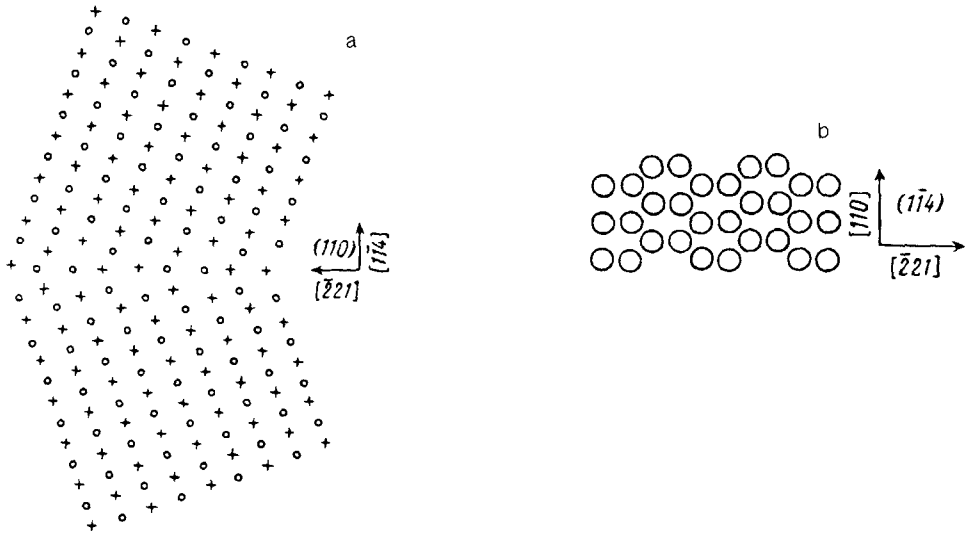


FIG. 3. Structure of a $\Sigma 9$ symmetric grain boundary in projection onto the (110) plane (a) and onto the (114) plane (b).

The components of the displacement along the $[\bar{2}\bar{2}1]$ direction lie in the interval $(1-8) \times 10^{-3}$, and those in the $[110]$ direction lie in the interval $(0-3) \times 10^{-3}$ nm. The average values of the displacements are two orders of magnitude smaller than the interplanar distances. This result indicates that the interaction with the atoms lying in the $(\bar{1}\bar{1}4)$ near-boundary planes is insignificant in the shaping of the atomic configuration of the $2(\bar{1}\bar{1}4)$ close-packed grain-boundary plane. This result supports the conclusion, reached in Ref. 9, that large-angle grain boundaries in metals can be treated as 2D ordered structures: 2D crystals with their characteristic structural defects.

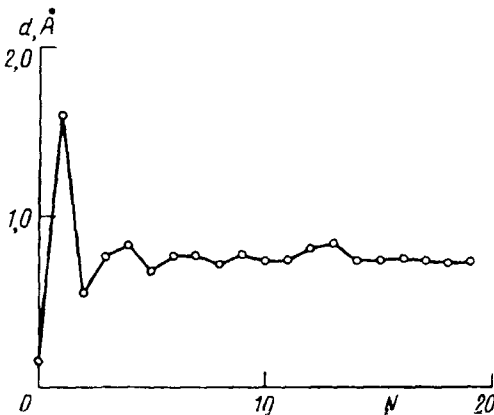


FIG. 4. Distance between $(\bar{1}\bar{1}4)$ planes versus the distance from the $\Sigma 9$ boundary.

The planar increase in the atomic density near the boundaries was observed both in an annealed tungsten wire and in a deformed (cold-drawn) wire. Some additional numerical simulations showed that the central plane remains close-packed at values of the rigid relative displacements of the lattice corresponding to nonequilibrium states of the boundary. One would thus expect the formation of close-packed atomic planes observed in this study to play an important role in structural conversions of boundaries which control the plastic deformation of polycrystalline samples. The oscillatory features in the fine structure of the near-boundary regions seen in the present study should have a substantial effect on the behavior of point defects. They may be responsible for the discrepancy between the diffusion width and the structural width of boundaries⁴ and for the oscillatory nature of the interaction of lattice dislocations with grain boundaries.¹⁰

This study was supported by the State Committee on Science and Technologies of the Ukraine and by the International Science Foundation.

¹S. E. Babcock and R. W. Baluffi, *Acta Metall.* **37**, 2367 (1989).

²V. S. Boiko *et al.*, *Vopr. At. Nauki Tekh. Ser. Fiz. Rad. Povrezhd. Rad. Mater.* **2**(44), 3 (1988).

³D. Wolf, *Acta Metall.* **38**, 791 (1990).

⁴I. M. Mikhailovskij *et al.*, *Phys. Status Solidi A* **125**, K65 (1991).

⁵B. S. Bokshtein *et al.*, *Structure and Properties of Internal Interfaces in Metals* [in Russian] (Nauka, Moscow, 1988).

⁶J. R. Smith and J. Ferrante, *Phys. Rev. B* **34**, 2238 (1986).

⁷E. W. Müller and T. T. Tzong, *Field Ion Microscopy* (American Elsevier, New York, 1969).

⁸R. A. Johnson and P. J. White, *Phys. Rev. B* **18**, 2939 (1978).

⁹P. A. Bereznyak *et al.*, *Vopr. At. Nauki Tekh. Ser. Fiz. Rad. Povrezhd. Rad. Mater.* **1**(43), 19 (1988).

¹⁰V. S. Boiko and I. N. Sidorenko, *Fiz. Met. Metalloved.* **67**, 444 (1989).

Translated by D. Parsons